

Detectability of the Order of Operations: An Information Theoretic Approach

Xiaoyu Chu, *Member, IEEE*, Yan Chen, *Senior Member, IEEE*, and K. J. Ray Liu, *Fellow, IEEE*

Abstract—As it is more and more convenient to manipulate multimedia content, the authenticity of multimedia content becomes questionable. While there are many forensic techniques developed to identify the use of a single manipulation operation, a few has considered the cases where multiple operations may be involved. In these cases, investigators not only need to identify the use of each operation, but also need to detect the order of these operations. However, due to the interplay among operations, the order of operations may not always be detectable. This leads to a fundamental question of when we can and cannot detect the order of operations. In this paper, we formulate the problem of detecting the order of operations as a multiple hypotheses testing problem. Then, we propose an information theoretical framework to model the relationship between the detected hypothesis and the true hypothesis. Under this framework, we propose a mutual information-based criterion to obtain the best detector and use it to determine whether we can or cannot detect the order of operations based on certain set of features. A case study of detecting the order of resizing and blurring has been examined to demonstrate the effectiveness of the proposed framework and criteria. In addition, two known forensic problems are considered in the simulations to show that the results obtained from the proposed framework and criteria match those of the existing works.

Index Terms—Order forensics, conditional fingerprints, mutual information, resizing and blurring.

I. INTRODUCTION

NOWADAYS, various editing software and online tools have been developed to retouch and manipulate digital multimedia content. Editing multimedia files becomes so easy and inexpensive that we can hardly trust the authenticity of multimedia content. However, since multimedia has been used as important evidence to make decisions or statements by authorities, such as law enforcement, news agency and government, it is critical to know whether the given multimedia content is trustful or maliciously tampered. To answer this question, many forensic techniques have been proposed to identify the use of different manipulation operations, such

as compression [1]–[3], resizing [4], [5], contrast enhancement [6], blurring [7]–[9] and so on [10]–[12].

Most of these techniques expose specific fingerprints of the considered operations and implicitly assume that no other operations were applied [1], [4]–[9], [11]. However, in reality, it is often the case that multiple operations are needed to complete a forgery. For example, if a forger wants to replace a person's face in an image using another person's face from another image, he or she may need to apply the following operations. First, the forger may need to apply resizing and contrast enhancement operations to the new face to make it match the size and color of the old face in the target image. Then, to avoid visible boundaries of the new face to the background of the target image, blurring may be applied to smooth the transition. At last, this forged image may be compressed for storage or transmission.

There have been some forensic techniques designed to identify the existence of a single operation in a certain operation chain [2], [3], [13]–[16]. Double compression detectors were developed to detect the existence of the first compression in a processing chain of two consecutive compressions [2], [3]. In [13], an improved double compression detector was proposed for the processing chain of two compressions with resizing in between. Specifically, two hypotheses were considered: whether the image was single JPEG compressed, or it was double JPEG compressed with resizing applied in the middle. Authors in [14] considered a similar scenario where linear contrast enhancement was interleaved with the two compressions. In addition, the contrast enhancement detector proposed in [15] can effectively detect this operation when it was applied to previously JPEG compressed images. Furthermore, authors in [16] are able to recover the compression history when full-frame linear filtering is applied after JPEG.

While these techniques considered multiple operations, their goal is to identify the existence of a specific operation in a certain processing chain. Nothing can be inferred about the order of operations from these techniques. However, when multiple different operations may be applied to the multimedia content, detecting the order of these operations is equally important with identifying the existence of each operation. By detecting the order of operations, we can obtain the complete processing history of multimedia content. Furthermore, given that different operations may be applied by different forgers, detecting the order may also help us identify who manipulated the multimedia content and when it was manipulated. For example, if investigators receive an image that was downloaded from the Internet and may be maliciously blurred by either the uploader or the downloader. Suppose that when an image is uploaded, resizing is needed to make the image fit

Manuscript received June 11, 2015; revised September 10, 2015, October 23, 2015, and December 12, 2015; accepted December 14, 2015. Date of publication December 22, 2015; date of current version February 1, 2016. This work was supported by the National Science Foundation under Grant CCF1320803. The associate editor coordinating the review of this manuscript and approving it for publication was Prof. Stefano Tubaro.

X. Chu was with the Department of Electrical and Computer Engineering, University of Maryland, College Park, MD 20742 USA. She is now with Google Inc., Mountain View, CA 94043 USA (e-mail: cxygrace@umd.edu).

Y. Chen is with the School of Electronic Engineering, University of Electronic Science and Technology of China, Chengdu 610051, China (e-mail: eecyan@uestc.edu.cn).

K. J. R. Liu is with the Department of Electrical and Computer Engineering, University of Maryland, College Park, MD 20742 USA (e-mail: kjrlu@umd.edu).

Color versions of one or more of the figures in this paper are available online at <http://ieeexplore.ieee.org>.

Digital Object Identifier 10.1109/TIFS.2015.2510958

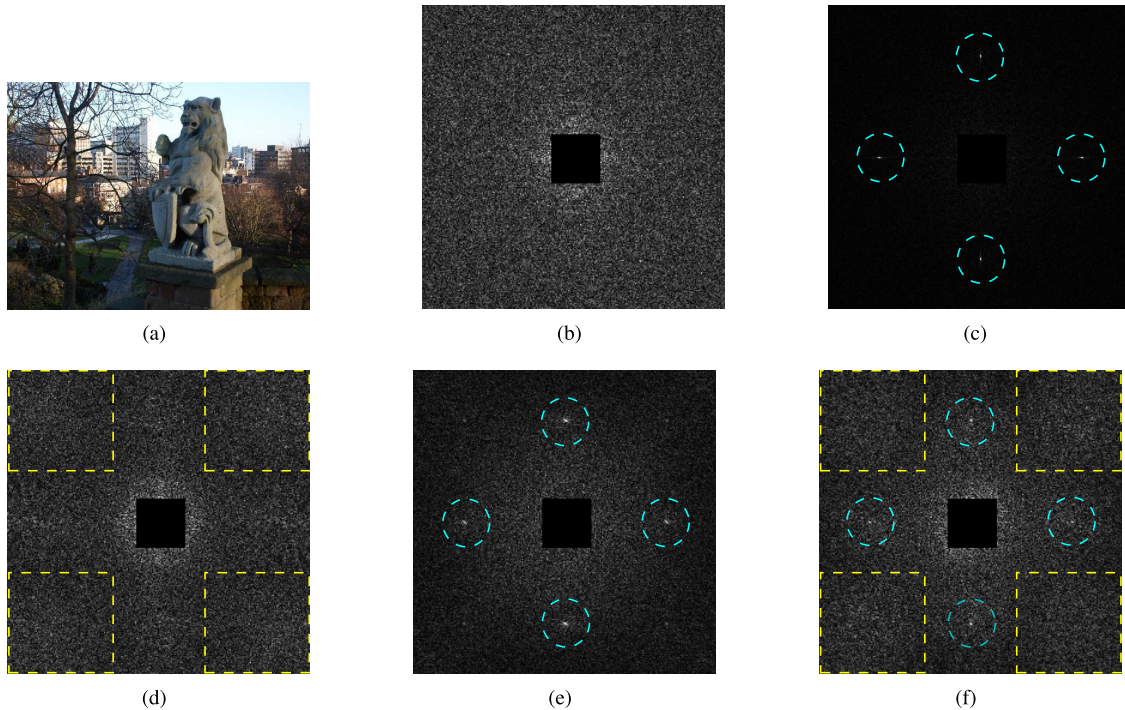


Fig. 1. Fingerprints for detecting the order of resizing and blurring. (a) and (b) are the original image and the DFT of its p-map, respectively. (c) - (f) show the DFT of the p-map of (c) the resized image, (d) the blurred image, (e) the blurred then resized image, and (f) the resized then blurred image. Resizing factor is 1.5 (upscaling). Gaussian blur is used with variance 1. Regions of interests are highlighted by dotted squares and circles.

the website standard. In this scenario, detecting the order of blurring and resizing can tell us who manipulated the image and when it was manipulated.

Few works have been done on detecting the order of operations. In [17], a forensic technique has been developed to detect the order of resizing and contrast enhancement. Nevertheless, the order of operations is not always detectable due to the interplay between operations. One reason would be that when multiple operations are applied to the multimedia content, later applied operations may affect, or even destroy, the fingerprints of earlier applied operations. For example, if JPEG compression or Gaussian noise is applied after contrast enhancement, the fingerprints of contrast enhancement would be too weak to be detected [15].

Therefore, a natural question would be “when can and cannot we detect the order of operations?” Authors in [18] have proposed two measures to determine the distinguishability of the order of operations when simple hypotheses are considered. In this work, we formulate the order detection problems into multiple hypotheses testing problems. For such problems, we propose an information theoretical framework by using mutual information based criteria to determine whether or not we can distinguish all considered hypotheses based on certain set of features. Furthermore, for those indistinguishable cases, this criterion can tell us which hypotheses are confused with each other and why they are confused. In addition, we also give a rigorous definition of the existence of conditional fingerprints. To verify the effectiveness of the proposed framework and criteria, we apply them to two known forensic problems to show that the obtained results match those published in existing works. Then, the proposed framework and criteria are applied to the problem of detecting

the order of resizing and blurring to obtain when we can or cannot detect their orders.

The remaining of this paper is organized as follows. Section II explains the fact that the order of operations is not always detectable and presents our system model for determining when they can or cannot be detected. The mutual information based criteria are proposed in Section III. Section IV presents our proposed detection scheme for detecting the order of resizing and blurring. To demonstrate the effectiveness of our proposed framework and criteria, Section V provides simulation results for both existing forensic problems and the problem examined in Section IV. Lastly, Section VI concludes our work.

II. SYSTEM MODEL

In this section, we first give an example to illustrate that the order of operations is not always detectable. Then, based on the analysis on the example, we propose an information theoretical framework for generalized multiple hypotheses testing problems.

A. Order of Operations May Not Be Detectable

When multiple operations are applied to multimedia content, the effect of later applied operations on earlier applied ones may lead to the undetectability of the order of operations. For example, let us consider a processing chain which may contain two operations: resizing and blurring. In order to identify the complete processing history, we need to detect not only the use of each operation, but also the order of them. Thus, the following five hypotheses are considered in the analysis

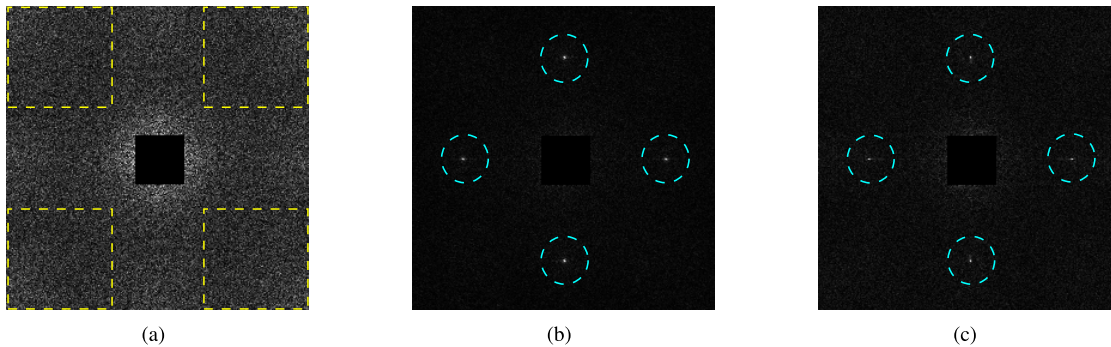


Fig. 2. A confusing example that we may not be able to detect the order. Plotted are DFTs of the p-map of (a) the blurred image, (b) the blurred then resized image, and (c) the resized then blurred image when resizing factor is 1.5 and the variance of Gaussian blur is 0.7. Regions of interests are highlighted by dotted squares and circles.

and needed to be distinguished.

$$\begin{aligned}
 H_0 &: \text{It is unaltered,} \\
 H_1 &: \text{It is altered by } A \text{ only,} \\
 H_2 &: \text{It is altered by } B \text{ only,} \\
 H_3 &: \text{It is altered by } B \text{ then } A, \\
 H_4 &: \text{It is altered by } A \text{ then } B,
 \end{aligned} \tag{1}$$

where A and B denote the operations of resizing and blurring respectively.

Figs. 1(b) - 1(f) show the different fingerprints of each hypothesis in the discrete Fourier transform (DFT) of an image's p-map. P-map is a probability matrix with each element representing the probability of the corresponding image pixel correlated with its neighbor pixels [4]. This matrix is widely used in detecting the resizing operation [5] because the linear interpolation process in resizing will lead to periodic characteristics of the p-map. Thus, when we take the DFT of the p-map, we would observe four distinct peaks in the corresponding spectrum, as they are shown in Fig. 1(c).

We assume that the blur operation is applied by using a linear filter on an image. Even though it does not give direct correlations between neighboring pixels, the neighbor pixels of a blurred image may still be correlated due to the overlapped dependency on the pixels of the original image. This alteration on pixel correlations caused by blurring may result in certain fingerprints in the p-map of the blurred image.

To see how pixel correlations are altered by blurring, we examined the p-map and its DFT of a blurred image. We have found that, in the DFT of the p-map, a blurred image has an increase of energy in high frequency component while the energy in the frequency domain of an unaltered image is monotonically decreasing as the frequency increases. We can see these fingerprints by comparing Fig. 1(d) with Fig. 1(b). These fingerprints can be used to detect blurring, as we will discuss in Section IV.

Furthermore, even when the image is previously resized, these fingerprints of blurring may still exist, as it is shown in Fig. 1(f). However, if resizing is applied after blurring, the fingerprints of blurring will be hardly detectable, as it is shown in Fig. 1(e). Nevertheless, either resizing then blurring or blurring then resizing, the DFT of the p-map is more noisy than that of the only resized case.

Based on the fingerprints of each hypothesis presented in Figs. 1(b) - 1(f), we can design algorithms to distinguish all hypotheses in (1) and thus detect the order of resizing and blurring. However, for some cases, these fingerprints are very weak and hardly detectable. Fig. 2 shows a confusing example where the same image in Fig. 1(a) was examined but the blurring effect is weaker than in Fig. 1. We can see that, though we may still be able to observe the fingerprints of blurring, we can hardly tell the difference between the blurred then resized image and the resized then blurred one. Therefore, in this case, we may not be able to detect the order of resizing and blurring.

B. Information Theoretical Model for Multiple Hypotheses Testing Problems

Given that the order of operations is not always detectable, a natural question would be "when can we and cannot we detect the order of operations?" To answer this question, we first consider a generalized multiple hypotheses testing problem as follows.

For forensic problems where we want to estimate the processing history of multimedia content, hypothesis test is commonly used. For example, in [5] of detecting resizing, two hypotheses were considered: H_0 , the image is unaltered; H_1 , the image is resized. In [17], five hypotheses were considered, similarly to those in (1) with B denoting the operation of contrast enhancement.

In order to distinguish these considered hypotheses, investigators go through the following typical steps [19]. First, possible fingerprints that can be used to distinguish each hypothesis are found. Then, based on these fingerprints, features are extracted from an examined image. At last, a set of detectors with tunable thresholds or parameters will be used to make the final decision of the detected hypothesis based on the extracted features. Fig. 3 shows this process.

Given certain features, detectors with different parameters will lead to different detection performance. For example, when detecting the resizing operation, simple hypothesis test was used [5]. Parameters of the detector determined the detection rate and false alarm rate. The overall performance of the detector can be measured by plotting a receiver operating characteristic (ROC) curve, which contains all reachable pairs of detection rates and false alarm rates.

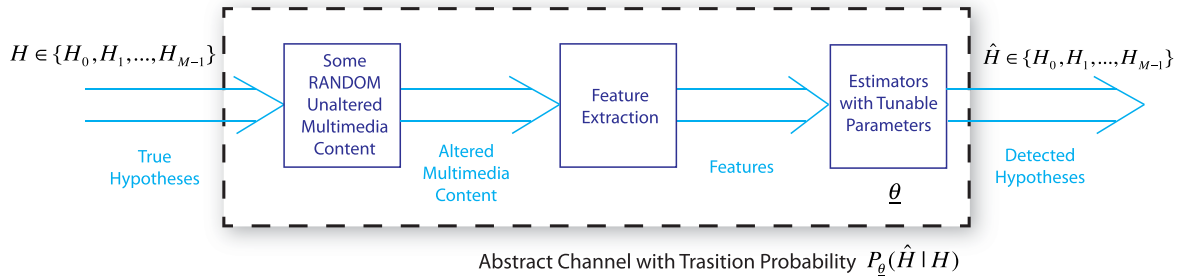


Fig. 3. A typical process of contrasting different hypotheses.

Let us consider another forensic problem where more than two hypotheses are involved. In [17] of detecting the order of resizing and contrast enhancement, five hypotheses were considered in the analysis. To demonstrate the detection performance, authors in [17] modified the ROC curves and plotted the curves of detection rate against the false discovery rate. Nevertheless, multiple curves were needed to show the detection performance.

This representation of multiple modified ROC curves could be problematic. Because when tuning the parameters, some curves may become better while others may be worse. It is hard to say which parameters yield the best overall detection performance.

In order to give a simple yet effective characterization, we use a transition probability matrix between the true hypotheses and the detected hypotheses to represent the performance of the detector with certain parameters. This representation is applicable for general multiple hypotheses testing problems. Furthermore, it can be used to compare the detection performance of different detectors, which will be discussed in the next section.

The transition probability matrix is defined as follows. Let $\mathcal{H} = \{H_0, H_1, \dots, H_{M-1}\}$ denote the set of considered hypotheses in a multiple hypotheses testing problem. Then the true hypothesis and the detected hypothesis, denoted as H and \hat{H} respectively, belong to this set. Based on certain features, a set of detectors with different parameters $\underline{\theta}$, denoted as $d_{\underline{\theta}}$, are used to contrast the different hypotheses. For each choice of $\underline{\theta}$, the performance of the specific detector is presented by a transition probability matrix $\mathbf{T}(\underline{\theta})$ with each element denoting the conditional probability of a detected hypothesis given a true hypothesis, i.e.,

$$\mathbf{T}_{i,j}(\underline{\theta}) = \mathbb{P}_{\underline{\theta}}(\hat{H} = H_j | H = H_i), \quad 0 \leq i, j < M. \quad (2)$$

With this definition, we propose a feature dependent abstract channel to characterize the relationship between true hypotheses and detected hypotheses. The channel characteristics, i.e., the transition probabilities between input and output (2), is specified by the parameters of the set of detectors, as it is shown in Fig. 3.

III. INFORMATION THEORETICAL CRITERIA

As we have formulated the order detection problem into a multiple hypotheses testing problem, our goal is to tell when we can and cannot distinguish all considered hypotheses based on certain features. Given that detectors with different parameters yield different detection performance, a natural thought would be to see if the best detector is able to distinguish all hypotheses. Then, the question becomes “which detector is the

best?” In this section, we first propose a mutual information criterion to determine the best detector. Then, based on this criterion, detection theoretical criteria will be used to determine when we can and cannot distinguish all hypotheses.

A. Mutual Information Criterion to Obtain the Best Detector

In the previous section, we have used a transition probability matrix to characterize the performance of a detector. The relationship between true hypotheses and detected hypotheses has been modeled as an abstract channel with transition probabilities $\mathbf{T}(\underline{\theta})$. Then, for the best detector, we would expect that the detected hypotheses contain the maximal information about the true hypotheses. Since mutual information is a measure of the information that the output of a channel contains about the input, we define the best detector based on this measure.

Definition 1: In a problem of detecting hypothesis $H \in \mathcal{H}$, detectors $d_{\underline{\theta}_1}$ and $d_{\underline{\theta}_2}$ are based on the same features. Let \hat{H} denote the detected hypothesis. $\mathbf{T}(\underline{\theta}_1)$ and $\mathbf{T}(\underline{\theta}_2)$ are transition probability matrices of detector $d_{\underline{\theta}_1}$ and $d_{\underline{\theta}_2}$, respectively. Let p_H denote the priors of H . Then, *detector $d_{\underline{\theta}_1}$ is better than $d_{\underline{\theta}_2}$, w.r.t. the mutual information criterion, when*

$$I_{p_H, \mathbf{T}(\underline{\theta}_1)}(H; \hat{H}) > I_{p_H, \mathbf{T}(\underline{\theta}_2)}(H; \hat{H}), \quad (3)$$

for the cases where we know the priors of H ; or

$$\max_{p_H} I_{p_H, \mathbf{T}(\underline{\theta}_1)}(H; \hat{H}) > \max_{p_H} I_{p_H, \mathbf{T}(\underline{\theta}_2)}(H; \hat{H}), \quad (4)$$

for the cases where we do not know the priors. $I(H; \hat{H})$ denotes the mutual information between H and \hat{H} .

This criterion compares the detection performance of different detectors based on the maximal information that detected hypotheses can possibly contain about true hypotheses by using a certain detector. Note that (3) is a special case of (4) when p_H is fixed. This criterion enables us to evaluate the best detector for general multiple hypotheses testing problems, especially when more than two hypotheses are considered. Furthermore, the properties of this measurement also match to those of the traditionally used ROC curves for simple hypothesis testing problems.

In order to show the effectiveness of our proposed mutual information criterion in simple hypothesis cases, we make a comparison between our information theoretical characterization of the detection performance and the traditional ROC curve, as it is shown in Fig. 4. In these cases, $\mathcal{H} = \{H_0, H_1\}$. Let p_d and p_f denote the detection rate and false alarm rate

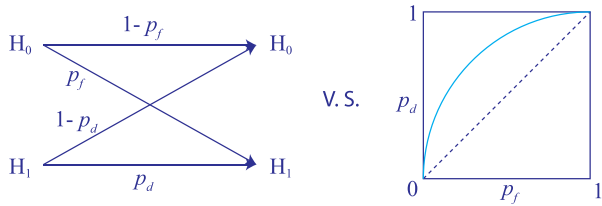


Fig. 4. Compare a simple hypothesis channel with a ROC curve.

as follows,

$$p_d = \mathbb{P}(\hat{H} = H_1 | H = H_1), \quad (5)$$

$$p_f = \mathbb{P}(\hat{H} = H_1 | H = H_0). \quad (6)$$

Given that uniform priors are usually implied when plotting ROC curves [12], we take $\mathbb{P}(H = H_0) = \mathbb{P}(H = H_1) = 1/2$.

The performance of a detector with a specific parameter $\underline{\theta}$ can be represented by either the value of mutual information $I_{p_H, \mathbf{T}(\underline{\theta})}(H; \hat{H})$ or a point (p_f, p_d) in the ROC curve. Because the mutual information only depends on p_d and p_f under the assumption of uniform priors, for comparison, we use a function $I(p_f, p_d)$ to denote the mutual information between H and \hat{H} . Then, we have the following properties of the mutual information criterion.

Lemma 1: For a simple hypothesis channel with uniform priors, the mutual information between H and \hat{H} , i.e., the function $I(p_f, p_d)$, has the following properties.

- 1) $I(p_f, p_d) = I(p_d, p_f)$
- 2) $p_{d1} > p_{d2} > p_f \Rightarrow I(p_f, p_{d1}) > I(p_f, p_{d2})$
- 3) $\arg \min_{p_f} I(p_f, p_d) = p_d$; $\arg \min_{p_d} I(p_f, p_d) = p_f$

Proof: Given the uniform priors and likelihood probabilities, we can obtain the probabilities of detected hypotheses as

$$\mathbb{P}(\hat{H} = H_0) = 1 - \frac{1}{2}(p_d + p_f), \quad (7)$$

$$\mathbb{P}(\hat{H} = H_1) = \frac{1}{2}(p_d + p_f). \quad (8)$$

Then, the mutual information for the simple hypothesis channel is

$$I(p_f, p_d) = h\left(\frac{1}{2}(p_d + p_f)\right) - \frac{1}{2}h(p_f) - \frac{1}{2}h(p_d), \quad (9)$$

where $h(p)$ denotes the binary entropy function of $(p, 1-p)$. From (9), we can see that $I(p_f, p_d)$ is a symmetric, i.e., $I(p_f, p_d) = I(p_d, p_f)$. Then, the first property is proved.

To prove the second property, we take the partial derivative of $I(p_f, p_d)$ w. r. t. p_d ,

$$\begin{aligned} \frac{\partial I(p_f, p_d)}{\partial p_d} &= -\frac{1}{2} \ln\left(\frac{1}{2}(p_d + p_f)\right) + \frac{1}{2} \ln\left(1 - \frac{1}{2}(p_d + p_f)\right) \\ &\quad + \frac{1}{2} \ln p_d - \frac{1}{2} \ln(1 - p_d) \\ &= \frac{1}{2} \ln\left(1 + \frac{p_d - p_f}{(p_d + p_f)(1 - p_d)}\right) \end{aligned} \quad (10)$$

Then, when $p_d \geq p_f$, the above derivative is greater than zero. Thus, for $p_d \geq p_f$, $I(p_f, p_d)$ is an increasing function of p_d . The second property is also proved.

Furthermore, we can also see from (10) that $p_d = p_f$ is the minimal of $I(p_f, p_d)$, i.e., $\arg \min_{p_d} I(p_f, p_d) = p_f$.

Similarly, we can also prove that $\arg \min_{p_f} I(p_f, p_d) = p_d$. Then, the last property is proved and it concludes our proof. ■

Since $I(p_f, p_d)$ measures the detection performance of a detector with detection rate p_d and false alarm rate p_f , it can also be interpreted as the measure of detection performance at a point (p_f, p_d) of a ROC curve. Then, the properties in lemma 1 can be interpreted in the following way.

- 1) Detection performance of each point in a ROC is symmetric along the random guess line $p_d = p_f$. This infers that, if our current detector is a point below this random guess line, we can simply invert all decisions of the detector to obtain its symmetric point above the line.
- 2) For points above the random guess line, given a certain false alarm rate, a detector with a higher detection rate is a better detector.
- 3) The worst performance is the random guess line.

We can easily see that the above properties match those in ROC curves.

Therefore, for simple hypothesis test cases, our proposed mutual information criterion is consistent with a ROC curve. Furthermore, the proposed criterion gives a way to evaluate the overall detection performance for cases where more than two hypotheses are considered. Our mutual information criterion is a general measurement of the detection performance for multiple hypotheses testing problems.

B. Detection Theoretical Criteria to Determine the Detectability of Multiple Hypotheses Testing Problems

By using the mutual information criterion, we can obtain the best detector and thus know how well investigators can achieve to contrast different hypotheses based on certain features. Furthermore, given the best detector, we can finally answer the question of when we can or cannot distinguish all considered hypotheses by checking if the best performed detector can distinguish all hypotheses. Specifically, if priors are uniform, we examine the likelihood probabilities of the best detector and check for each true hypothesis, if the detection probability is greater than any misdetection probabilities. If nonuniform priors are assumed or we do not know the priors, we examine the posterior probabilities of the best detector.

Definition 2: For a multiple hypotheses testing problem, where considered hypotheses are $\mathcal{H} = \{H_0, H_1, \dots, H_{M-1}\}$, let H and \hat{H} denote the true hypothesis and the detected hypothesis, respectively. Assume that priors are positive. Then, under the mutual information criterion, all hypotheses can be distinguished by detectors $d_{\underline{\theta}}, \underline{\theta} \in \mathbb{R}^k$, if and only if the following conditions are satisfied.

- If priors are uniform, the conditions are

$$\mathbb{P}_{\underline{\theta}^*}(\hat{H} = H_i | H = H_i) > \mathbb{P}_{\underline{\theta}^*}(\hat{H} = H_j | H = H_i) + \delta_{i,j},$$
 for any $i, j = 0, 1, \dots, M-1$, and $i \neq j$; (11)
- If priors are nonuniform or unknown, the conditions are

$$\mathbb{P}_{\underline{\theta}^*}(H = H_i | \hat{H} = H_i) > \mathbb{P}_{\underline{\theta}^*}(H = H_j | \hat{H} = H_i) + \delta_{i,j},$$
 for any $i, j = 0, 1, \dots, M-1$, and $i \neq j$, (12)

and

$$\mathbb{P}_{\underline{\theta}^*}(\hat{H} = H_i) > \epsilon, \quad \forall i = 0, 1, \dots, M-1, \quad (13)$$

where $\delta_{i,j} \geq 0$ are confidence factors indicating how well the hypothesis can be distinguished from others. ϵ is a small positive constant and $\underline{\theta}^*$ are parameters of the best detector w.r.t. the mutual information criterion. That is, if we know the priors,

$$\underline{\theta}^* = \arg \max_{\underline{\theta}} I_{p_H, \mathbf{T}(\underline{\theta})}(H; \hat{H}). \quad (14)$$

If we do not know the priors,

$$(\underline{\theta}^*, p_H^*) = \arg \max_{\underline{\theta}, p_H} I_{p_H, \mathbf{T}(\underline{\theta})}(H; \hat{H}). \quad (15)$$

Note that for cases of unknown priors, the above definition of distinguishability cannot guarantee that the best detector can distinguish the hypotheses for any priors. However, this definition can be easily extended for cases where we have more information about the priors.

Furthermore, by examining the conditions in (11) and (12), we are able to tell which hypotheses are confused with each other when we cannot distinguish all hypotheses.

Definition 3: For the problem in Definition 2, two hypotheses, H_i and H_j , $i \neq j$, are confused with each other when the following conditions meet.

- If priors are uniform,

$$\mathbb{P}_{\underline{\theta}^*}(\hat{H} = H_i | H = H_i) \leq \mathbb{P}_{\underline{\theta}^*}(\hat{H} = H_j | H = H_i) + \delta_{i,j},$$

or,

$$\mathbb{P}_{\underline{\theta}^*}(\hat{H} = H_j | H = H_j) \leq \mathbb{P}_{\underline{\theta}^*}(\hat{H} = H_i | H = H_j) + \delta_{j,i}.$$

- If priors are nonuniform or unknown,

$$\mathbb{P}_{\underline{\theta}^*}(H = H_i | \hat{H} = H_i) \leq \mathbb{P}_{\underline{\theta}^*}(H = H_j | \hat{H} = H_i) + \delta_{i,j},$$

or,

$$\mathbb{P}_{\underline{\theta}^*}(H = H_j | \hat{H} = H_j) \leq \mathbb{P}_{\underline{\theta}^*}(H = H_i | \hat{H} = H_j) + \delta_{j,i}.$$

The reason of why hypotheses may be confused with each other is related to the strength of fingerprints or conditional fingerprints [17]. As our examples in (1) and at the beginning of Section II-B show, each hypothesis represents an operation chain. This operation chain can be an empty chain which denotes the hypothesis of unaltered multimedia content. It can also be a single operation chain or a multiple operations chain. We first define fingerprints and conditional fingerprints of operation chains as follows.

Definition 4: Consider an operation chain and its corresponding hypothesis, denoted as \underline{S}_i and H_i respectively. Let $\underline{S}_{\emptyset}$ and H_{\emptyset} denote the empty operation chain, and the hypothesis of unaltered multimedia content. If $\underline{S}_i \neq \underline{S}_{\emptyset}$, then the fingerprints of \underline{S}_i are a set of features that can be used to distinguish $\{H_i, H_{\emptyset}\}$. Next, we consider another operation chain, denoted as \underline{S}_j . If \underline{S}_i is a sub-chain of \underline{S}_j , let $\underline{S}_{j \setminus i}$ denote the operation chain of \underline{S}_j excluding \underline{S}_i . $H_{j \setminus i}$ is denoted as the corresponding hypothesis of $\underline{S}_{j \setminus i}$. Then, the conditional fingerprints of \underline{S}_i given \underline{S}_j are a set of features that can be used to distinguish the following hypotheses:

$$\{H_{j \setminus i}, H_i, H_j\}.$$

Remarks: To better understand the difference between fingerprints and conditional fingerprints, we give the following example. Let \underline{S}_i and \underline{S}_j denote the operation chain of only

contrast enhancement and contrast enhancement then resizing, respectively. Then, $\underline{S}_{j \setminus i}$ represents the operation chain of only resizing. When detecting contrast enhancement, the fingerprints we commonly used are the high frequency components of the DFT of the pixel histogram [6]. However, these cannot be the conditional fingerprints of contrast enhancement given contrast enhancement then resizing [17]. This is because that resized images and contrast enhanced then resized images, i.e., $\{H_{j \setminus i}, H_j\}$, cannot be distinguished by examining the fingerprints of contrast enhancement. In [17], the conditional fingerprints of contrast enhancement given contrast enhancement then resizing are two features. One is the maximum gradient of the periodogram of the Fourier transformed p-map, which is the fingerprint of resizing. The other feature is the distance of normalized histograms between the full image and the down-sampled image [17]. By using these two features, we can distinguish resized images, contrast enhanced images, and contrast enhanced then resized images, i.e., $\{H_{j \setminus i}, H_i, H_j\}$.

Based on fingerprints and conditional fingerprints, forensic techniques can be designed to detect operations and their orders [12], [17]. Similarly, in a multiple hypotheses testing problem, the existence of required fingerprints and conditional fingerprints enables us to distinguish all hypotheses. Based on Definition 3, rigorous definitions of the existence of fingerprints and conditional fingerprints can be obtained as follows.

Definition 5: Consider a multiple hypotheses testing problem where $\mathcal{H} = \{H_0, H_1, \dots, H_{M-1}\}$. Let H_{\emptyset} denote the empty chain hypothesis. For a hypothesis $H_i \in \mathcal{H}$, $H_i \neq H_{\emptyset}$, let \underline{S}_i denote the processing chain represented by this hypothesis. Then, the fingerprints of \underline{S}_i exist if

H_i is not confused with H_{\emptyset} by Definition 3.

Now, consider another hypothesis H_j , $j \neq i$ and $H_j \neq H_{\emptyset}$, the processing chain it represents is \underline{S}_j . The fingerprints of \underline{S}_i and \underline{S}_j are different if

H_i is not confused with H_j by Definition 3.

Furthermore, if \underline{S}_i is a sub-chain of \underline{S}_j , let $H_{j \setminus i}$ denote the hypothesis representing $\underline{S}_{j \setminus i}$, then the conditional fingerprints of \underline{S}_i given \underline{S}_j exist if

any two of $\{H_{j \setminus i}, H_i, H_j\}$ are not confused by Definition 3.

Having all concepts defined for general hypotheses testing problems, let us examine the special cases of detecting the order of operations where five hypotheses are considered in the analysis (1). Then, the order of A and B can be detected if and only if we can distinguish all hypotheses in (1) by Definition 2. This requires that any two hypotheses cannot be confused with each other by Definition 3. That is, the following conditions on fingerprints and conditional fingerprints should hold by Definition 5.

- Fingerprints of A , B , $A \rightarrow B$, and $B \rightarrow A$ exist.
- Conditional Fingerprints of A given $A \rightarrow B$ exist.
- Conditional Fingerprints of B given $B \rightarrow A$ exist.
- Fingerprints of $A \rightarrow B$ and $B \rightarrow A$ are different.

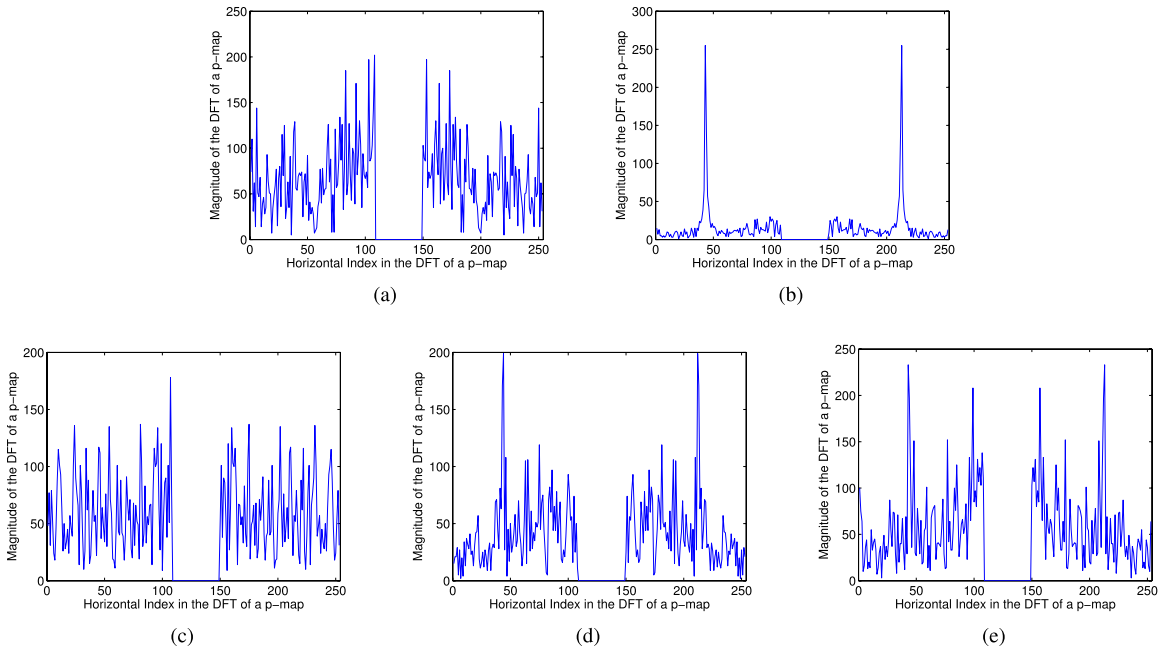


Fig. 5. The central horizontal line of the DFT of the p-map of (a) an unaltered image, (b) a resized image, (c) a blurred image, (d) a blurred then resized image, and (e) a resized then blurred image.

IV. DETECTING THE ORDER OF RESIZING AND BLURRING

To demonstrate the effectiveness of the proposed framework and criteria, we consider a case study of detecting the order of resizing and blurring. In this problem, we are distinguishing the five hypotheses in (1). Thus, this is a multiple hypotheses testing problem and can be analyzed using our information theoretical framework.

As we have shown in Fig. 1, each of the five hypotheses has its unique fingerprints in the DFT of an image’s p-map, which may help us contrast these hypotheses. Based on these fingerprints, we take two features to distinguish these hypotheses. One feature is to detect the existence of four peaks and measure the strength of these peaks. The other feature is to capture the increase of noise energy in high frequency regions.

A. Feature 1: PSNR

In order to measure the strength of the peaks with respect to noise nearby, we use a peak signal to noise ratio (PSNR) feature which calculates the ratio of the peak value to the mean of the absolute value of noise close to this peak. To obtain this measure, we first extract the central horizontal lines of the DFT of the p-maps from Figs 1(b)-1(f) and plot the magnitude versus the horizontal index of each pixel on these lines in Figs 5(a)-5(e), respectively. By appropriately choosing thresholds, this measure can be used to categorize the five hypotheses into three classes: unaltered or only blurred images; blurred then resized or resized then blurred images; only resized images.

Specifically, let us take the resized then blurred case as an example, i.e., the signal in Fig. 5(d). Given the symmetry of the signal, we first consider the left half of the signal. Let y_l and x denote the magnitude and the index, respectively. Since the noise mean increases with the index, we first use the following linear regression model to make the noise mean

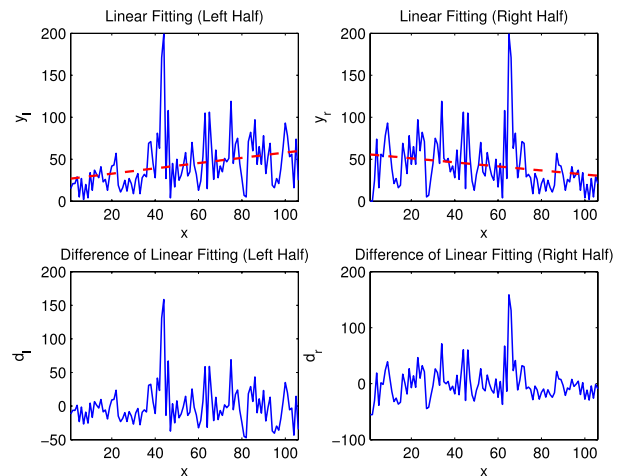


Fig. 6. The process of how to calculate the PSNR from the central horizontal line of the DFT of a p-map. Take Fig. 5(d) as an example.

uniform so that the peak is more prominent.

$$y_l = a_1x + b_1 + n. \tag{16}$$

An example of the linear regression process is shown in the upper left figure of Fig. 6. After estimating the parameters as \hat{a}_1 and \hat{b}_1 by least squares, we obtain the difference signal

$$d_l = y_l - \hat{a}_1x - \hat{b}_1, \tag{17}$$

as it is shown in the bottom left figure of Fig. 6.

Then, the peak is detected from d_l by finding the coordinates of its maximum value (x_p, y_p) . From the bottom left figure in Fig. 6 we can see that, the noise variance changes a lot as it is farther from the peak. Thus, instead of calculating the mean of the absolute value of noise in the whole range,

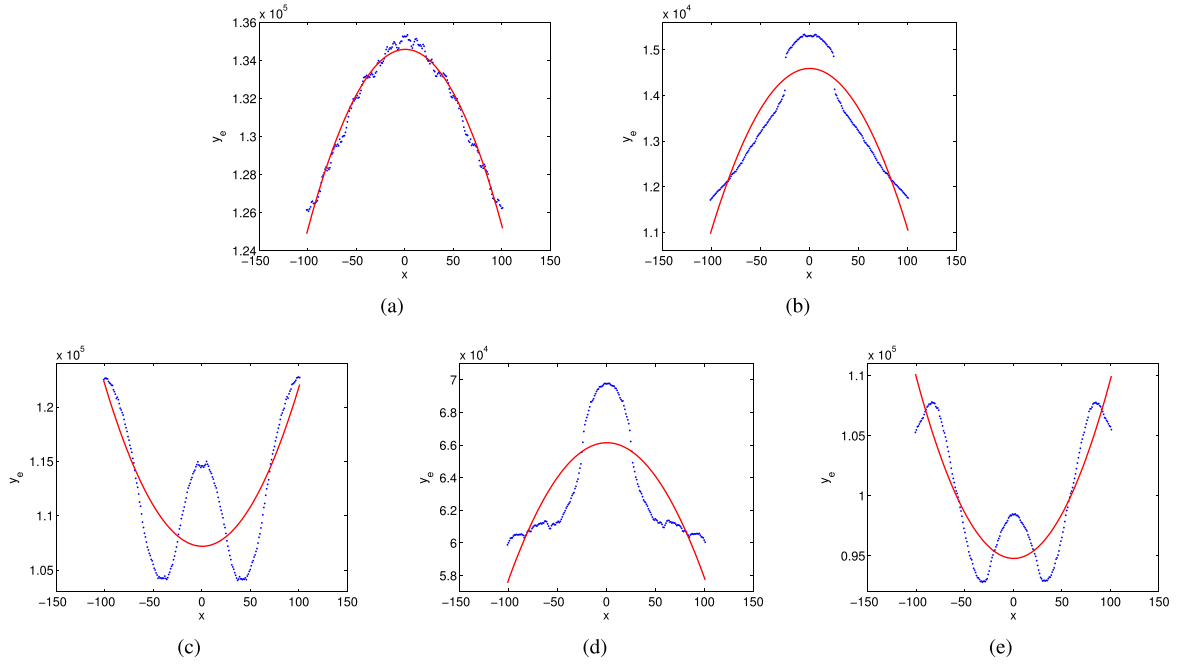


Fig. 7. The noise energy pattern signal (dotted blue lines) extracted from the DFT of the p-map and their polynomial fitting curves (solid red lines) for (a) an unaltered image, (b) a resized image, (c) a blurred image, (d) a blurred then resized image, and (e) a resized then blurred image.

we only consider the regions close to the peak. Then, PSNR is calculated as follows.

$$\text{PSNR}_l = \frac{y_p}{\text{mean}_{0 < |x-x_p| < \varepsilon} (|d_l(x)|)}. \quad (18)$$

Similar process is then applied to the right half of the signal in Fig. 5(d) to obtain PSNR_r . Then, the PSNR measurement for the central horizontal line of the DFT of a p-map is

$$\text{PSNR}_h = \max(\text{PSNR}_l, \text{PSNR}_r). \quad (19)$$

Given that the peaks also present in the central vertical line of the DFT of the p-map, we calculate the above PSNR measurement, denoted as PSNR_v , for the central vertical line signal as well. Then, the first PSNR feature used to distinguish hypotheses in (1) is

$$\text{PSNR} = \max(\text{PSNR}_h, \text{PSNR}_v). \quad (20)$$

We can make the following detection based on this feature,

$$\hat{H} = \begin{cases} H_0 \text{ or } H_2, & \text{if } \text{PSNR} < \tau_1, \\ H_3 \text{ or } H_4, & \text{if } \tau_1 \leq \text{PSNR} < \tau_2, \\ H_1, & \text{if } \text{PSNR} \geq \tau_2, \end{cases} \quad (21)$$

where τ_1 and τ_2 are tunable parameters.

B. Feature 2: Noise Energy Pattern

To further distinguish H_2 from H_0 and H_4 from H_3 , we examine the fingerprints of blurring. As shown in Fig. 1(d) and Fig. 1(f), when blurring is applied as the last operation, we would observe an increase of noise energy at high frequencies of the DFT of the p-map. In order to capture this change of noise energy, we calculate a noise energy pattern signal near the boundaries of the DFT of a p-map.

Specifically, let $Z = \{Z_{m,n}\}$ denote the magnitudes of the DFT of a p-map. The origin is located at the upper left corner of the matrix with size a by a . The noise energy signal, which is denoted as a matrix E , is first calculated as a summation of neighboring magnitudes in Z , i.e.,

$$E = Z \otimes \mathbf{1}_w, \quad (22)$$

where $\mathbf{1}_w$ is an all one matrix of size w by w , and \otimes is a convolution operator. Then, we take a one dimensional signal y_e near the boundaries of E as the noise energy pattern signal:

$$y_e(x) = \frac{(E_{v,a/2+x} + E_{a/2+x,a-v} + E_{a-v,a/2-x} + E_{a/2-x,v})}{4}, \quad (23)$$

where $v - a/2 \leq x < a/2 - v$ and $v = \lceil w/2 \rceil + 1$.

In Figs 7(a)-7(e), the dotted blue lines are noise energy pattern signals for the DFT of the p-maps in Figs 1(b)-1(f), respectively. We can see that the fingerprints of blurring result in an increase of the noise energy with $|x|$ for higher values of $|x|$, as shown in Figs 7(c) and 7(e). To measure these fingerprints, we use a second order polynomial model to fit the signal as

$$y_e = a_2x^2 + b_2x + c_2, \quad (24)$$

and see if the estimated function is convex or concave. The solid red lines in Fig. 7 are the estimated curves. If the estimated \hat{a}_2 is positive, then the noise energy pattern signal is estimated as a convex function. This indicates that the noise energy tends to increase with $|x|$ for higher $|x|$'s. Thus blurring fingerprints are detected. Otherwise, if the estimated function is concave, blurring fingerprints are not detected. The detection

we can make by this feature is

$$\hat{H} = \begin{cases} H_0 \text{ or } H_1 \text{ or } H_3, & \text{if } \hat{a}_2 < 0, \\ H_2 \text{ or } H_4, & \text{if } \hat{a}_2 > 0. \end{cases} \quad (25)$$

Combining the detection results from (21) and (25), our decision rule of the proposed detector for detecting the order of resizing and blurring is

$$\hat{H} = \begin{cases} H_0, & \text{if } \text{PSNR} < \tau_1 \text{ and } \hat{a}_2 < 0, \\ H_1, & \text{if } \text{PSNR} \geq \tau_2, \\ H_2, & \text{if } \text{PSNR} < \tau_1 \text{ and } \hat{a}_2 > 0, \\ H_3, & \text{if } \tau_1 \leq \text{PSNR} < \tau_2 \text{ and } \hat{a}_2 < 0, \\ H_4, & \text{if } \tau_1 \leq \text{PSNR} < \tau_2 \text{ and } \hat{a}_2 > 0. \end{cases} \quad (26)$$

In our proposed algorithm, the detection has two tunable parameters, and thus $\underline{\theta} = (\tau_1, \tau_2)$. Given the detector and its parameters, we will apply our mutual information based criteria to simulation results to answer the question of “when can we and cannot we detect the order of resizing and blurring” in Section V-C.

V. SIMULATION RESULTS

In this section, we conduct several simulations to demonstrate the effectiveness of our information theoretical framework and mutual information based criteria. We first examine two existing forensic problems, one simple hypothesis problem and one order detection problem, to verify the correctness of our framework and criteria. Then, the detection of the order of resizing and blurring is examined to show when we can and cannot detect the order of these two operations.

A. Detect Double JPEG Compression

Since our framework and criteria can be used for general multiple hypotheses testing problems, we start with a well-known simple hypothesis testing problem in forensics, double JPEG compression detection [2], [3], [20]–[23]. We want to prove that the results obtained from our method match those from published literature.

To detect double JPEG compression, two hypotheses are considered in the analysis:

$$\begin{aligned} H_0 &: \text{The image is single JPEG compressed,} \\ H_1 &: \text{The image is double JPEG compressed.} \end{aligned} \quad (27)$$

There are many features that can be used to distinguish these hypotheses [2], [3], [20], [22]. All of them can yield over 90% detection rates for most JPEG compression quality factors. While our framework can be applied to any features and corresponding detectors, we use the first digit feature of DCT coefficients as an example to see if the results obtained from our framework match those in the existing work [3].

The detector in [3] was proposed based on the double JPEG compression fingerprints in the first digit of DCT coefficients. Specifically, If an image is single JPEG compressed, the first digit of its DCT coefficients obeys a general Benford’s law:

$$p(d) = N \log_{10} \left(1 + \frac{1}{s + dq} \right), \quad d \in \{1, 2, \dots, 9\}, \quad (28)$$

where s and q are model parameters and N is a normalization factor. The first digit d of a non-zero integer x is computed as

$$d = \left\lfloor \frac{x}{10^{\lfloor \log_{10} x \rfloor}} \right\rfloor, \quad (29)$$

where $\lfloor \cdot \rfloor$ is the floor rounding operation. If the image is double JPEG compressed, however, this law will not hold for the first digit of its DCT coefficients.

Given these fingerprints, a detector for distinguishing hypotheses in (27) can be designed as follows. First, we obtain the normalized histogram of the first digit of DCT coefficients. Then, we use these statistics to estimate the general Benford’s law and calculate the sum of squared errors (SSE) between the estimated distribution and the normalized histogram. The final decision is made by comparing the mean SSE of the 20 lowest frequency subbands with a tunable threshold θ as follows [3],

$$\hat{H} = \begin{cases} H_0, & \text{if } \text{mean SSE} < \theta, \\ H_1, & \text{if } \text{mean SSE} \geq \theta. \end{cases} \quad (30)$$

In order to determine whether we can detect double JPEG compression, we first generate a testing database using the 1338 unaltered images from the UCID database [24]. Specifically, these images are first JPEG compressed by quality factors from 50 to 95 with step size of 5 to obtain the single JPEG compressed image database. Then, each of the image in this database is re-compressed by the same set of quality factors to compose the double JPEG compressed image database. Let Q_1 and Q_2 denote the quality factors used in the first and second JPEG compression, respectively. Then, for each pair of Q_1 and Q_2 , the testing database contains 1338 single compressed images using Q_2 and 1338 double compressed images using Q_1 then Q_2 .

We first assume uniform priors for the two hypotheses as most literatures do [3], [22]. Then, using (3) in Definition 1, we can obtain the best parameter θ^* that yield the highest mutual information between the detected hypotheses and the true hypotheses. By checking the conditions (11) in Definition 2, we determine whether we can distinguish these two hypotheses for a given pair of Q_1 and Q_2 . Unless specified otherwise, we use confidence factors $\delta_{i,j} = 0$ in simulations. The results of all combinations of Q_1 and Q_2 are shown in Fig. 8(a).

We can see that for most cases, double JPEG compression can be detected by using the proposed model. This matches the results in [3].

For indistinguishable cases, confused hypotheses are H_0 and H_1 by Definition 3. This means that the conditional fingerprints of JPEG compression given the operation chain of double JPEG compression do not exist in these cases by Definition 5. Specifically, this is because 1) $Q_1 = Q_2$, though there are other features that can be used to deal with this situation [23]; 2) the secondary quantization step size is a multiple integer of the first quantization step size for most of the extracted DCT subbands.

Note that we may be able to distinguish more cases if using a support vector machine (SVM) as the detector and tune the position of the hyperplane as the parameters [3].

Then, we consider a general case where we do not know the priors of the two hypotheses. The best detector would be determined by (4) in Definition 1 and we should use the criterion (12) in Definition 2 to determine whether we can

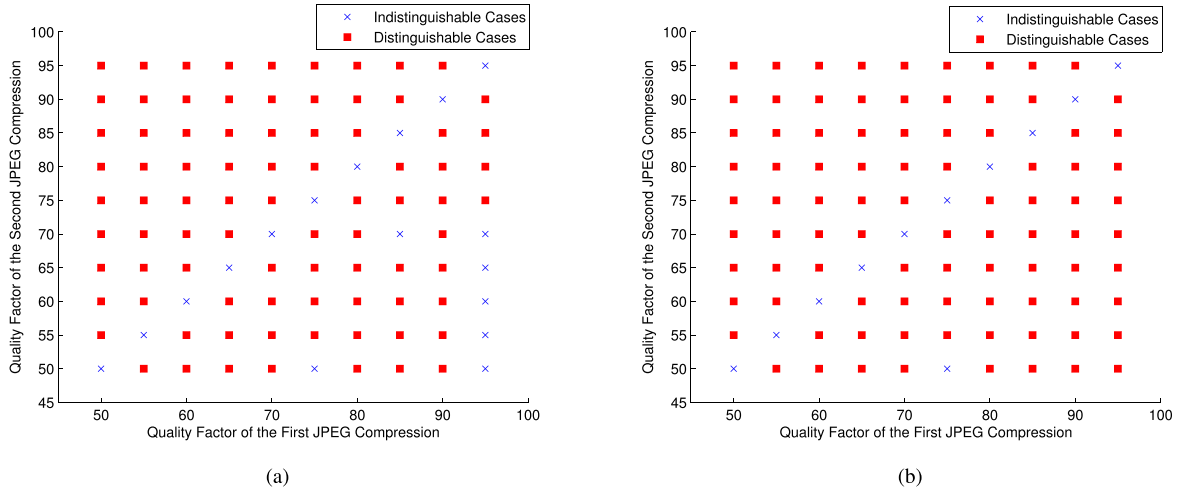


Fig. 8. Distinguishability test results of detecting double JPEG compression by applying our information theoretical framework and criteria. (a) Priors are known and uniform. (b) Priors are unknown.

distinguish the hypotheses. Fig. 8(b) shows the results under this assumption.

Since there are fewer constraints on the priors in the case of unknown priors, the best detector can yield higher mutual information in this case than that of the uniform priors case. Then, the best detection performance we can get from unknown priors would be better than that from the uniform priors. Therefore, we have more distinguishable cases in Fig. 8(b) than those in Fig. 8(a). In other words, the reason that some scenarios are detectable in the case of unknown priors but not in the case of known priors is that, the priors which make the scenario detectable in the case of unknown priors may not be those considered in the case of known priors.

B. Detect the Order of Resizing and Contrast Enhancement

The next case study we examine is the order detection of resizing and contrast enhancement, which contains more than two hypotheses [17]. In this forensic problem, five hypotheses are considered and needed to be distinguished as in (1) with A and B denoting resizing and contrast enhancement.

The fingerprints of H_3 and H_4 were found in [17] as follows. If an image is first resized then contrast enhanced, both fingerprints of resizing and contrast enhancement can be revealed from the image. However, if an image is first contrast enhanced then resized, only the fingerprints of resizing can be revealed. Nevertheless, we can still detect the previously applied contrast enhancement by examining a down-sampled image of the resized image. This is because that, if the resizing factor can be represented as a rational number $s = a/b$ such that $a, b \in \mathbb{N}$ and are mutually prime, then every a pixel in the resized image will occur at the same spatial location as a pixel in the original image. Therefore, the resizing operation can be reverse engineered by down-sampling the image with factor $1/a$. If contrast enhancement is previously applied, then its fingerprints can be revealed from this down-sampled image.

Given these fingerprints, a tree structured detection scheme was proposed in [17]. First, resizing fingerprints are examined [5]. In this step, the feature extracted is the maximum derivative of the cumulative periodogram calculated from the DFT of the p-map. We denote this feature as f_{rs} . If f_{rs} is

greater than a threshold, denoted as α , it means that resizing has been applied to this image. Thus, we can detect the hypothesis as one of $\{H_1, H_3, H_4\}$. Otherwise, the image belongs to either H_0 or H_2 .

If resizing fingerprints have been detected from the image, then we can use the conditional fingerprints of contrast enhancement given contrast enhancement then resizing to detect the previously applied contrast enhancement [17]. The feature extracted is the distance of normalized pixel histograms between the full image and the down-sampled image with factor $1/a$. To obtain a , the resizing factor needs to be estimated [25], which involves the use of a training database and SVM. Let f_{cers} denote the feature extracted in this step. If f_{cers} is greater than a threshold λ , then previously applied contrast enhancement is detected in the resized image. Thus, the detected hypothesis is H_3 . Otherwise, the image belongs to either H_1 or H_4 .

To distinguish H_2 from H_0 or H_4 from H_1 , the fingerprints of contrast enhancement are examined [6]. The feature is taken from the high frequency components of the DFT of the normalized pixel histogram. Let f_{ce} denote this feature. To distinguish $\{H_0, H_2\}$, if f_{ce} is greater than a threshold β_1 , then the image is detected as H_2 . Otherwise, it is detected as H_0 . Similar decision is applied for distinguishing $\{H_1, H_4\}$, whose threshold is denoted as β_2 .

In summary, the detection algorithm is as follows.

$$\hat{H} = \begin{cases} H_0, & \text{if } f_{rs} < \alpha \text{ and } f_{ce} < \beta_1, \\ H_1, & \text{if } f_{rs} \geq \alpha, f_{cers} < \lambda \text{ and } f_{ce} < \beta_2, \\ H_2, & \text{if } f_{rs} < \alpha \text{ and } f_{ce} > \beta_1, \\ H_3, & \text{if } f_{rs} \geq \alpha \text{ and } f_{cers} \geq \lambda, \\ H_4, & \text{if } f_{rs} \geq \alpha, f_{cers} < \lambda \text{ and } f_{ce} > \beta_2, \end{cases} \quad (31)$$

There are four tunable parameters and thus $\underline{\theta} = (\alpha, \lambda, \beta_1, \beta_2)$.

In order to know when we can and cannot detect the order of resizing and contrast enhancement, we use 1000 images from the UCID database to generate our test database. The rest 338 images are used to generate the training database for the resizing factor estimation step. We use gamma corrections with parameter γ to simulate the contrast

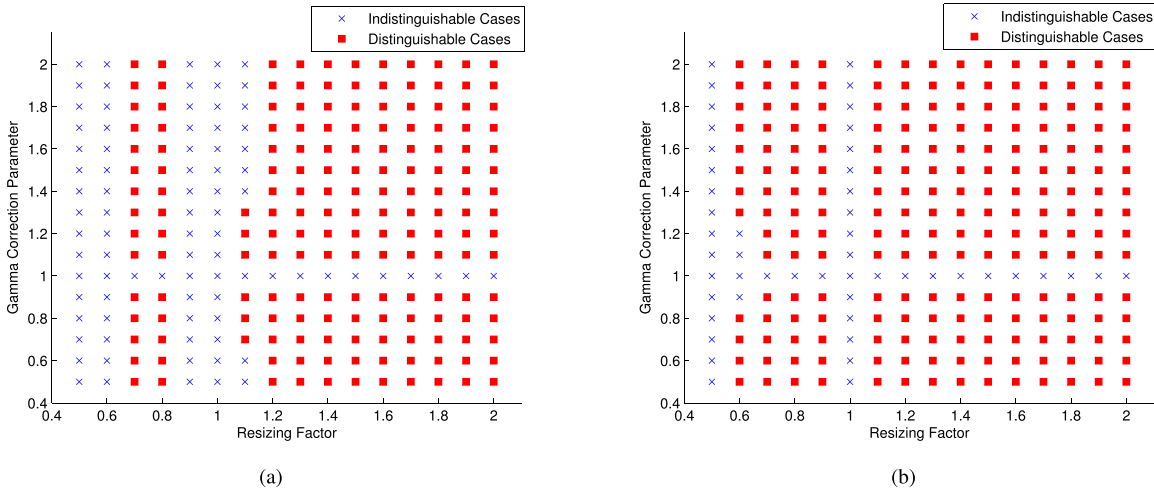


Fig. 9. Distinguishability test results of detecting the order of resizing and contrast enhancement by applying our information theoretical framework and criteria. (a) Priors are known and uniform. (b) Priors are unknown.

enhancement operation [6]. For each $\gamma \in \{0.5, 0.6, \dots, 2\}$ and $s \in \{0.5, 0.6, \dots, 2\}$, the test database contains: 1000 unaltered images, 1000 resized images with scaling factor s , 1000 contrast enhanced images with gamma correction parameter γ , 1000 contrast enhanced then resized images, and 1000 resized then contrast enhanced images. Note that for $\gamma = 1$ or $s = 1$, contrast enhancement or resizing is not actually applied. Thus, we cannot distinguish all five hypotheses in these cases. To estimate the resizing factor, the training database for SVM contains 5070 ($=338 \times 15$) images whose resizing factors are taken from $\{0.5, 0.6, \dots, 0.9, 1.1, \dots, 2\}$ [25].

We still consider two cases regarding the priors of the considered hypotheses. For uniform priors, the simulation results are shown in Fig. 9(a). While for the cases that we do not know priors, the results are shown in Fig. 9(b). As expected, when we do not have constraints on priors of the hypotheses, we have more distinguishable cases than that when uniform priors are assumed.

In [17], two examples of resizing factors and gamma correction parameters, ($s = 1.5, \gamma = 0.5$) and ($s = 1.25, \gamma = 0.7$), are examined in experiments. Specific detection performance for these two pairs of parameters are plotted in five ROC curves. In both cases, authors in [17] have shown that the proposed detector can successfully detect the order of resizing and contrast enhancement. To compare these results with those obtained by our framework, let us examine the uniform priors case. From Fig. 9(a), we can see that ($s = 1.5, \gamma = 0.5$) and the four neighbors of ($s = 1.25, \gamma = 0.7$) are distinguishable points. We conducted an additional experiment on ($s = 1.25, \gamma = 0.7$) and found that this point is also distinguishable. This shows that the results obtained by our approach match those in [17].

Besides the two example cases examined in [17], we obtain the detectability results for the whole range of resizing factors and gamma correction parameters. From these results, we have found that, though we can detect the order of resizing and contrast enhancement for most of the cases, there are a few indistinguishable cases. We examine these cases and use Definition 3 to find which hypotheses are confused to make it indistinguishable. In addition, the reasons of why

these hypotheses are confused is summarized as follows by Definition 5.

- H_2 is confused with H_4 for the indistinguishable cases where $s = 1.1$. This means that the conditional fingerprints of resizing given resizing then contrast enhanced do not exist in these scenarios. The effect of later applied contrast enhancement on the fingerprints of previously applied resizing is more obvious as the strength of contrast enhancement increases, i.e., for larger values of $|\gamma - 1|$.
- H_3 is confused with H_1 or H_4 when $s = 0.6, 0.9$. Given the tree structure of the detection algorithm, this is due to the failure of distinguishing H_3 from H_1 and H_4 by the conditional fingerprints of contrast enhancement given contrast enhancement then resizing. This conditional fingerprints do not exist for these scenarios either because of the incorrect estimation of the resizing factor or due to the insufficient number of pixels extracted from the down-sampled image.

C. Detect the Order of Resizing and Blurring

By applying our information theoretical framework and criteria to double JPEG compression detection and the order detection of resizing and contrast enhancement, we have shown that the results obtained from our proposed framework match those in existing works. In this section, we examine the order detection of resizing and blurring and find when we can and cannot detect the order of these two operations.

For forensic problems examined in previous Sections V-A and V-B, the considered hypotheses can be distinguished for most of the cases. However, as we have shown in Fig. 2, there are some cases where the fingerprints of resizing then blurring and those of blurring then resizing are very similar. In these cases, the order of resizing and blurring may not be detectable according to Definition 2 with confidence factors $\delta_{i,j} = 0$. Then, our framework and criteria can be used to determine when this order can or cannot be detected.

In this experiment, we use all 1338 unaltered images in UCID database to generate the test database. We use Gaussian

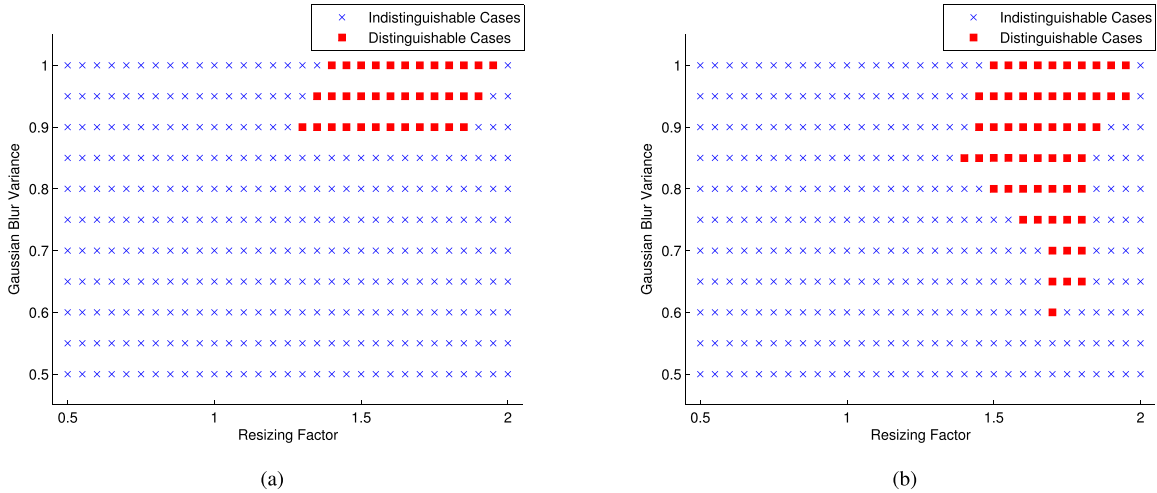


Fig. 10. Distinguishability test results of detecting the order of resizing and blurring by applying our information theoretical framework and criteria. (a) Priors are known and uniform. (b) Priors are unknown.

TABLE I

POSTERIOR PROBABILITIES USED BY DEFINITION 2 TO DETERMINE THE DISTINGUISHABILITY OF DETECTING THE ORDER OF RESIZING AND BLURRING WHEN RESIZING FACTOR IS 1.5, AND (A) GAUSSIAN BLUR VARIANCE IS 1 AND (B) GAUSSIAN BLUR VARIANCE IS 0.7. H_0, H_1, \dots, H_4 ARE DEFINED IN (1). THE NUMBER IN CELL ($\hat{H} = H_i, H = H_j$) DENOTES THE POSTERIOR PROBABILITY $\mathbb{P}_{\theta^*}(H = H_j | \hat{H} = H_i)$. THE CELL IN GREEN INDICATES THE MAXIMUM POSTERIOR PROBABILITY IN THE ROW

(A)

	$H = H_0$	$H = H_1$	$H = H_2$	$H = H_3$	$H = H_4$
$\hat{H} = H_0$	0.7268	0	0.1798	0.0189	0.0746
$\hat{H} = H_1$	0	0.9575	0	0.0394	0.0031
$\hat{H} = H_2$	0.0071	0	0.9889	0	0.0040
$\hat{H} = H_3$	0.0156	0.0089	0.0089	0.8943	0.0722
$\hat{H} = H_4$	0	0	0.0510	0.0425	0.9066

(B)

	$H = H_0$	$H = H_1$	$H = H_2$	$H = H_3$	$H = H_4$
$\hat{H} = H_0$	0.7148	0	0.2800	0.0052	0
$\hat{H} = H_1$	0	0.7903	0	0.0739	0.1358
$\hat{H} = H_2$	0.0462	0	0.9538	0	0
$\hat{H} = H_3$	0.0022	0.1697	0.0043	0.3702	0.4536
$\hat{H} = H_4$	0	0	0	0.0159	0.9841

blur with filter window 5 by 5 and variance ν to simulate the blurring operation. For each $s = \{0.5, 0.55, \dots, 2\}$ and $\nu = \{0.5, 0.55, \dots, 1\}$, the test database contains: 1338 unaltered images, 1338 resized images with scaling factor s , 1338 blurred images with Gaussian variance ν , 1338 blurred then resized images, and 1338 resized then blurred images. The reasonable range of $\nu \leq 1$ is obtained by calculating the distortion introduced by blurring using the structure similarity (SSIM) index [26] and then setting the reasonable SSIM values to be greater than 0.9.

Based on the detector proposed in Section IV with tunable parameters $\underline{\theta} = (\tau_1, \tau_2)$ (26), we use our information theoretical framework and criteria to obtain the distinguishable and indistinguishable cases for different pairs of s and ν .

We first examine the two examples presented in Section II-A where resizing factor is 1.5 and Gaussian blur variances are 1 and 0.7 respectively. Table I lists the posterior probabilities used by Definition 2 to determine the distinguishabilities of detecting the order of resizing and blurring when priors are

unknown for these two cases. We can see that in Table I(A), the maximum posterior in each row locates at the diagonal line of the table. This means that $\forall i, j, i \neq j, \mathbb{P}_{\theta^*}(H = H_i | \hat{H} = H_i) > \mathbb{P}_{\theta^*}(H = H_j | \hat{H} = H_i)$. Thus, according to Definition 2, the order can be detected in this case.

For the other case where Gaussian blur variance is 0.7, Table I(B) shows that not all maximum posteriors are along the diagonal line of the table. Thus, the order cannot be detected in this case. Furthermore, the exception happens when $\mathbb{P}_{\theta^*}(H = H_4 | \hat{H} = H_3) > \mathbb{P}_{\theta^*}(H = H_3 | \hat{H} = H_3)$. According to Definition 3, this indicates that the confusing hypotheses which make the order undetectable are H_3 and H_4 . This matches the results shown in Fig. 2 where the fingerprints of blurring then resizing and resizing then blurring are similar and can be hardly distinguished.

Then, following the same procedure, we obtain the distinguishabilities of all considered s and ν and plot them in Fig. 10. Fig. 10(a) shows results for the case of uniform priors and Fig. 10(b) considers the case where priors are unknown. Due to the fewer constraints on hypothesis priors, Fig. 10(b) contains more distinguishable cases than Fig. 10(a) does.

To further understand why we cannot detect the order of resizing and blurring in those indistinguishable cases, we examine the transition scenarios where distinguishable cases becomes indistinguishable. That is, we analyze the indistinguishable cases close to the range of distinguishable cases in Fig. 10. By Definition 3, we have found that for most cases, the confusing hypotheses that makes the order undetectable are H_3 and H_4 in (1). Thus, by Definition 5, the reason that we cannot detect the order of resizing and blurring in these cases is that the fingerprints of blurring then resizing and resizing then blurring are the same. This matches the example we have shown in Fig. 2 where the fingerprints in Fig. 2(b) and Fig. 2(c) are similar.

In addition, we consider a scenario where manipulations are applied to a compressed image. Then, more than two operations are involved in the analysis. In this scenario, investigators obtain a JPEG image, and want to distinguish the following hypotheses:

H_0 : It is single compressed,

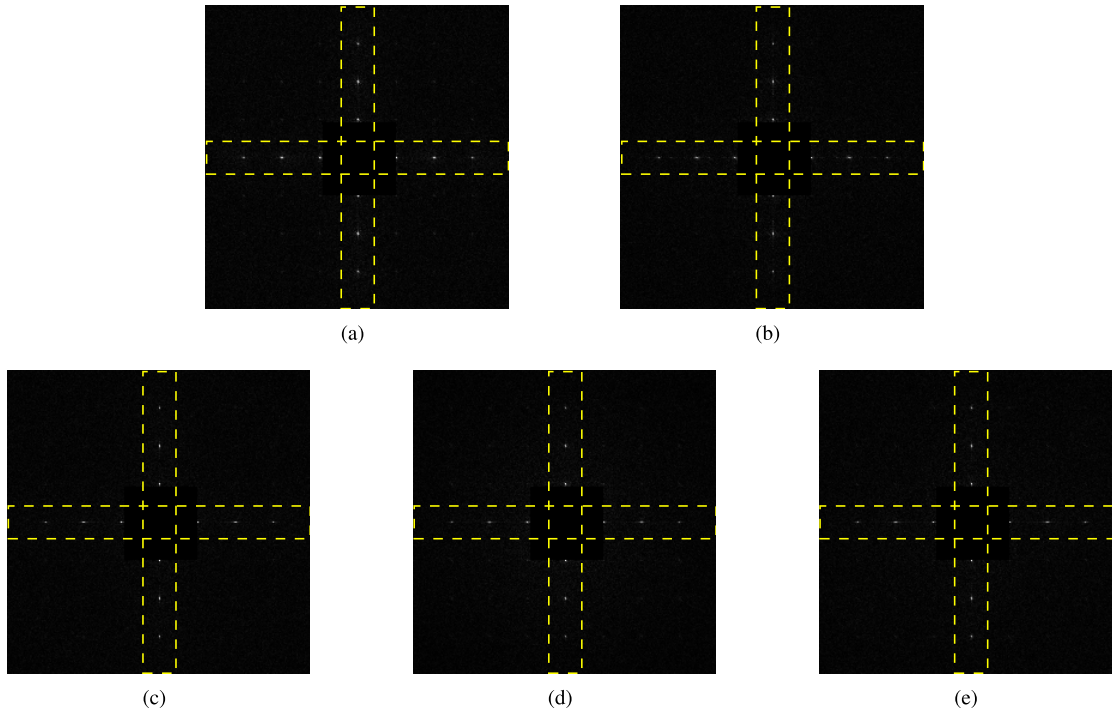


Fig. 11. The DFT of the p-map of (a) a single JPEG compressed image with compression quality factor 75, and (b)-(e) double JPEG compressed images with compression quality factors 75 then 85 and interleaved by (b) resizing, (c) blurring, (d) blurring then resizing, and (e) resizing then blurring. The same image in Fig. 1(a) is examined in this example. Resizing factor is 1.5 and the variance of Gaussian blur is 1. Regions of interests are highlighted by dotted rectangles.

- $$\begin{aligned}
 H_1 &: \text{It is double compressed interleaved by resizing,} \\
 H_2 &: \text{It is double compressed interleaved by blurring,} \\
 H_3 &: \text{It is double compressed interleaved by} \\
 &\quad \text{blurring then resizing,} \\
 H_4 &: \text{It is double compressed interleaved by} \\
 &\quad \text{resizing then blurring.}
 \end{aligned} \tag{32}$$

Fig. 11 shows the DFT of the p-map for each of the hypotheses. Since the blocking artifact also results in peaks in the DFT of the p-map, both fingerprints of resizing and blurring are weakened by the last applied JPEG compression. Thus, these five hypotheses are easily confused with each other and may not be distinguishable based on p-map related features.

We want to note that, our framework and the mutual information based criterion can be applied to any chosen features. Furthermore, by comparing the maximum mutual information that each set of features can achieve, one can determine the best set of features within the candidate feature sets based on our proposed criterion.

VI. CONCLUSION

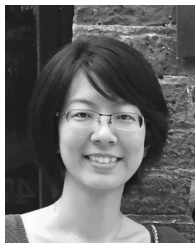
In this paper, we proposed an information theoretical framework and mutual information based criteria to answer the question of when we can or cannot detect the order of operations. Specifically, we first formulated the order detection problems into multiple hypotheses testing problems. Then, based on a certain set of detectors, mutual information based criteria were proposed to determine whether we can distinguish all considered hypotheses. To demonstrate the effectiveness of our

proposed framework and criteria, we first apply them to two existing and detectable problems: double JPEG compression detection and the order detection of resizing and contrast enhancement. Simulations show that the results obtained by our framework match with those from existing literatures. Then, the case study of detecting the order of resizing and blurring is examined, where the order may not always be detectable. In this case study, we proposed a detection technique to detect their order. Based on this detector, we used our information theoretical framework and criteria to obtain the detectable cases and find the reasons for undetectable cases.

REFERENCES

- [1] Z. Fan and R. L. de Queiroz, "Identification of bitmap compression history: JPEG detection and quantizer estimation," *IEEE Trans. Image Process.*, vol. 12, no. 2, pp. 230–235, Feb. 2003.
- [2] A. C. Popescu and H. Farid, "Statistical tools for digital forensics," in *Proc. 6th Int. Workshop Inf. Hiding*, Toronto, ON, Canada, 2004, pp. 128–147.
- [3] B. Li, Y. Q. Shi, and J. Huang, "Detecting doubly compressed JPEG images by using mode based first digit features," in *Proc. IEEE 10th Workshop Multimedia Signal Process.*, Oct. 2008, pp. 730–735.
- [4] A. C. Popescu and H. Farid, "Exposing digital forgeries by detecting traces of resampling," *IEEE Trans. Signal Process.*, vol. 53, no. 2, pp. 758–767, Feb. 2005.
- [5] M. Kirchner, "Fast and reliable resampling detection by spectral analysis of fixed linear predictor residue," in *Proc. 10th ACM Workshop Multimedia Secur.*, New York, NY, USA, 2008, pp. 11–20.
- [6] M. C. Stamm and K. J. R. Liu, "Forensic detection of image manipulation using statistical intrinsic fingerprints," *IEEE Trans. Inf. Forensics Security*, vol. 5, no. 3, pp. 492–506, Sep. 2010.
- [7] H. Tong, M. Li, H. Zhang, and C. Zhang, "Blur detection for digital images using wavelet transform," in *Proc. IEEE Int. Conf. Multimedia Expo (ICME)*, vol. 1, Jun. 2004, pp. 17–20.

- [8] G. Cao, Y. Zhao, and R. Ni, "Edge-based blur metric for tamper detection," *J. Inf. Hiding Multimedia Signal Process.*, vol. 1, no. 1, pp. 20–27, Jan. 2010.
- [9] B. Su, S. Lu, and C. L. Tan, "Blurred image region detection and classification," in *Proc. 19th ACM Int. Conf. Multimedia*, New York, NY, USA, 2011, pp. 1397–1400.
- [10] X. Chu, M. C. Stamm, and K. J. R. Liu, "Compressive sensing forensics," *IEEE Trans. Inf. Forensics Security*, vol. 10, no. 7, pp. 1416–1431, Jul. 2015.
- [11] M. C. Stamm, W. S. Lin, and K. J. R. Liu, "Temporal forensics and anti-forensics for motion compensated video," *IEEE Trans. Inf. Forensics Security*, vol. 7, no. 4, pp. 1315–1329, Aug. 2012.
- [12] M. C. Stamm, M. Wu, and K. J. R. Liu, "Information forensics: An overview of the first decade," *IEEE Access*, vol. 1, pp. 167–200, 2013.
- [13] T. Bianchi and A. Piva, "Reverse engineering of double JPEG compression in the presence of image resizing," in *Proc. IEEE Int. Workshop Inf. Forensics Secur.*, Dec. 2012, pp. 127–132.
- [14] P. Ferrara, T. Bianchi, A. De Rosa, and A. Piva, "Reverse engineering of double compressed images in the presence of contrast enhancement," in *Proc. IEEE 15th Int. Workshop Multimedia Signal Process.*, Sep./Oct. 2013, pp. 141–146.
- [15] G. Cao, Y. Zhao, R. Ni, and X. Li, "Contrast enhancement-based forensics in digital images," *IEEE Trans. Inf. Forensics Security*, vol. 9, no. 3, pp. 515–525, Mar. 2014.
- [16] V. Conotter, P. Comesana, and F. Pérez-González, "Forensic detection of processing operator chains: Recovering the history of filtered JPEG images," *IEEE Trans. Inf. Forensics Security*, vol. 10, no. 11, pp. 2257–2269, Nov. 2015.
- [17] M. C. Stamm, X. Chu, and K. J. R. Liu, "Forensically determining the order of signal processing operations," in *Proc. IEEE Int. Workshop Inf. Forensics Secur.*, Nov. 2013, pp. 162–167.
- [18] P. Comesana and F. Pérez-González, "Multimedia operator chain topology and ordering estimation based on detection and information theoretic tools," in *Proc. 11th Int. Conf. Digit. Forensics Watermarking*, Berlin, Germany, 2013, pp. 213–227.
- [19] X. Chu, Y. Chen, M. C. Stamm, and K. J. R. Liu, "Information theoretical limit of compression forensics," in *Proc. IEEE Int. Conf. Acoust., Speech, Signal Process.*, May 2014, pp. 2689–2693.
- [20] Y.-L. Chen and C.-T. Hsu, "Detecting doubly compressed images based on quantization noise model and image restoration," in *Proc. IEEE Int. Workshop Multimedia Signal Process.*, Oct. 2009, pp. 1–6.
- [21] X. Feng and G. Doërr, "JPEG recompression detection," *Proc. SPIE, Media Forensics Secur.*, vol. 7541, pp. 0J1–0J10, Feb. 2010.
- [22] T. Pevný and J. Fridrich, "Detection of double-compression in JPEG images for applications in steganography," *IEEE Trans. Inf. Forensics Security*, vol. 3, no. 2, pp. 247–258, Jun. 2008.
- [23] F. Huang, J. Huang, and Y. Q. Shi, "Detecting double JPEG compression with the same quantization matrix," *IEEE Trans. Inf. Forensics Security*, vol. 5, no. 4, pp. 848–856, Dec. 2010.
- [24] G. Schaefer and M. Stich, "UCID: An uncompressed color image database," *Proc. SPIE, Storage Retr. Methods Appl. Multimedia*, vol. 5307, pp. 472–480, Jan. 2004.
- [25] S. Pfennig and M. Kirchner, "Spectral methods to determine the exact scaling factor of resampled digital images," in *Proc. 5th Int. Symp. Commun. Control Signal Process.*, May 2012, pp. 1–6.
- [26] Z. Wang, A. C. Bovik, H. R. Sheikh, and E. P. Simoncelli, "Image quality assessment: From error visibility to structural similarity," *IEEE Trans. Image Process.*, vol. 13, no. 4, pp. 600–612, Apr. 2004.



Xiaoyu Chu (S'11–M'15) received the B.S. degree in electrical engineering from Shanghai Jiao Tong University, Shanghai, China, in 2010, and the Ph.D. degree in electrical engineering from the University of Maryland, College Park, in 2015. She is currently a Senior Software Engineer with Google Inc., Mountain View, CA.

Her research interests include signal processing, information security, multimedia forensics, and anti-forensics.

Ms. Chu was a recipient of the First Prize in the 22nd Chinese Physics Olympiad, the Best Thesis Award of Shanghai Jiao Tong University, the Honor of Excellent Graduate of Shanghai Jiao Tong University, and the University of Maryland Future Faculty Fellowship in 2013.



Yan Chen (SM'14) received the bachelor's degree from the University of Science and Technology of China, in 2004, the M.Phil. degree from the Hong Kong University of Science and Technology, in 2007, and the Ph.D. degree from the University of Maryland, College Park, MD, USA, in 2011. Being a Founding Member, he joined Origin Wireless Inc. as a Principal Technologist in 2013. He is currently a Professor with the University of Electronic Science and Technology of China. His research interests include data science, network science, game theory, social learning, and networking, as well as signal processing and wireless communications.

He was a recipient of multiple honors and awards, including the best paper award at the IEEE GLOBECOM in 2013, the Future Faculty Fellowship and the Distinguished Dissertation Fellowship Honorable Mention from the Department of Electrical and Computer Engineering in 2010 and 2011, the Finalist of the Dean's Doctoral Research Award from the A. James Clark School of Engineering, University of Maryland in 2011, and the Chinese Government Award for outstanding students abroad in 2010.



K. J. Ray Liu (F'03) was named a Distinguished Scholar-Teacher with the University of Maryland, College Park, in 2007, where he is a Christine Kim Eminent Professor of Information Technology. He leads the Maryland Signals and Information Group conducting research encompassing broad areas of information and communications technology with recent focus on future wireless technologies, network science, and information forensics and security.

Dr. Liu was a recipient of the 2016 IEEE Leon K. Kirchmayer Technical Field Award on graduate teaching and mentoring, the IEEE Signal Processing Society 2014 Society Award, and the IEEE Signal Processing Society 2009 Technical Achievement Award. Recognized by Thomson Reuters as a Highly Cited Researcher, he is a fellow of AAAS.

Dr. Liu is a member of the IEEE Board of Directors. He was the President of the IEEE Signal Processing Society, where he has served as the Vice President Publications and on the Board of Governors. He has also served as the Editor-in-Chief of the *IEEE Signal Processing Magazine*.

He also received teaching and research recognitions from the University of Maryland, including the University-Level Invention of the Year Award; and the College-Level Poole and Kent Senior Faculty Teaching Award, the Outstanding Faculty Research Award, and the Outstanding Faculty Service Award, all from the A. James Clark School of Engineering.